

## Comparative studies on as-cast microstructures and mechanical properties between Mg–3Ce–1.2Mn–0.9Sc and Mg–3Ce–1.2Mn–1Zn magnesium alloys

YANG Ming-bo<sup>1,2,3</sup>, PAN Fu-sheng<sup>3</sup>

1. Materials Science and Engineering College, Chongqing University of Technology, Chongqing 400054, China;

2. Key Laboratory of Automobile Components Manufacturing and Testing Technology of Ministry of Education, Chongqing University of Technology, Chongqing 400054, China;

3. National Engineering Research Center for Magnesium Alloys, Chongqing University, Chongqing 400030, China

Received 24 December 2010; accepted 15 April 2011

**Abstract:** The as-cast microstructures and mechanical properties of Mg–3Ce–1.2Mn–0.9Sc and Mg–3Ce–1.2Mn–1Zn magnesium alloys were investigated and compared. The results indicate that the Sc-containing alloy mainly consists of  $\alpha$ -Mg, Mg<sub>12</sub>Ce and Mn<sub>2</sub>Sc phases, and the Zn-containing alloy is mainly composed of  $\alpha$ -Mg and Mg<sub>12</sub>Ce phases. The morphologies of the Mg<sub>12</sub>Ce phases in the two as-cast alloys are different. The Mg<sub>12</sub>Ce phases in the Sc- and Zn-containing alloys mainly exhibit particle-like shapes and continuous and/or quasi-continuous nets, respectively. Furthermore, the grains of the Sc-containing alloy are finer than those of the Zn-containing alloy. In addition, the Sc- and Zn-containing alloys have similar as-cast tensile properties at room temperature and 300 °C. However, the Sc-containing alloy exhibits higher creep-resistant properties at 300 °C and 30 MPa for 100 h than the Zn-containing alloy.

**Key words:** magnesium alloy; Mg–Ce–Mn based alloys; Sc; Zn; Mg<sub>12</sub>Ce phase

### 1 Introduction

At present, the development of new magnesium alloys is becoming increasingly important due to the potential saving in mass compared with aluminum based alloys. However, the creep properties of magnesium alloys are limited by their low melting point which can vary depending on the alloying content [1]. Hence, the development of elevated temperature magnesium alloys is necessary in order to compete with other light constructional materials such as aluminum alloys and in order to improve the temperature range of application of magnesium components. Previous investigations indicated that magnesium alloys based on the Mg–Sc system exhibited interesting properties [2–4], and it was further found that the addition of Mn and Ce to Mg–Sc alloys could improve the creep resistance substantially [5, 6]. For example, the quaternary Mg–Ce–Mn–Sc alloys are considerably superior to WE alloys and exhibit high creep resistance at high temperatures over 300 °C [6, 7].

However, due to the expensive scandium, the application of the Mg–Ce–Mn–Sc alloys is limited. Therefore, the research of replacing expensive scandium by cheap alloying elements for the Mg–Ce–Mn–Sc alloys needs to be considered. Since Zn can form intermetallic phases with Mg and/or RE as plates on basal planes of  $\alpha$ -Mg matrix and SMOLA et al [8] found that the Mg–4Y–1Mn–1Zn alloy exhibited higher creep-resistant properties than the Mg–4Y–1Mn–1Sc alloy. It is inferred that Zn is the possible less expensive alternative to Sc in the Mg–Ce–Mn–Sc alloys. However, the available information whether Sc in the Mg–Ce–Mn–Sc alloys can be replaced, especially the information concerning the comparison of microstructures and mechanical properties of the Mg–Ce–Mn–Sc and Mg–Ce–Mn–Zn alloys, is very scarce at present. Due to the above mentioned-reasons, the present work is to investigate and compare the as-cast microstructures and mechanical properties of the Mg–3Ce–1.2Mn–0.9Sc and Mg–3Ce–1.2Mn–1Zn magnesium alloys.

**Foundation item:** Project (50725413) supported by the National Natural Science Foundation of China; Project (2007CB613704) supported by the National Basic Research Program of China; Projects (2010AC4085, 2009AB4134) supported by the Chongqing Science and Technology Commission of China; Project (2010CSTC-HDLS) supported by the Program for Hundreds of Distinguished Leading Scientists of CQ CSTC, China

**Corresponding author:** YANG Ming-bo; Tel: +86-23-62563176; E-mail: yangmingbo@cqut.edu.cn  
DOI: 10.1016/S1003-6326(11)61139-4

## 2 Experimental

The nominal compositions (mass fraction, %) of the experimental alloys investigated in this work were Mg–3Ce–1.2Mn–0.9Sc (1<sup>#</sup> alloy) and Mg–3Ce–1.2Mn–1Zn (2<sup>#</sup> alloy). The experimental alloys were prepared by adding pure Mg, pure Zn, Mg–29%Ce, Mg–2.91%Sc and Mg–4.38%Mn master alloys. The experimental alloys were melted in a crucible resistance furnace and protected by the RJ–2 flux additions (45% MgCl<sub>2</sub>+37% KCl+8% NaCl+4% CaF<sub>2</sub>+6% BaCl<sub>2</sub>). After being held at 740 °C for 60 min, the melts of the experimental alloys were homogenized by mechanical stirring and then poured into a permanent mould which was coated and preheated to 200 °C in order to obtain a casting. The specimens shown in Fig. 1 were fabricated from the castings for tensile and creep tests. Furthermore, the samples of the experimental alloys were subjected to a solution heat treatment (520 °C, 12 h+water cooling) in order to clearly reveal the grain boundaries.

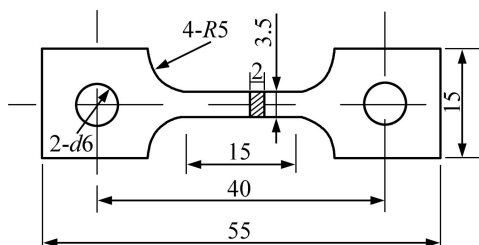


**Fig. 1** Configuration of samples used for tensile and creep tests (unit: mm)

The as-cast and solutionized samples of the experimental alloys were respectively etched in an 8% nitric acid solution in distilled water and a solution of 1.5 g picric, 25 mL ethanol, 5 mL acetic acid and 10 mL distilled water, and then examined by an Olympus optical microscope and JOEL JSM–6460LV type scanning electron microscope equipped with Oxford energy dispersive X-ray spectrometer (EDS) with an operating voltage of 20 kV. The grain size was analyzed by the standard linear intercept method using an Olympus stereomicroscope. The phases in the experimental alloys were also analyzed by D/Max–1200X type analyzer operated at 40 kV and 30 mA.

The as-cast tensile properties of the experimental alloys at room temperature and 300 °C were determined from a complete stress–strain curve. Ultimate tensile strength (UTS), 0.2% yield strength (YS), and elongation to failure (Elong.) were obtained based on the average value of three tests. Constant-load tensile creep tests were performed at 300 °C and 30 MPa for creep extension up to 100 h. The minimum creep rates of

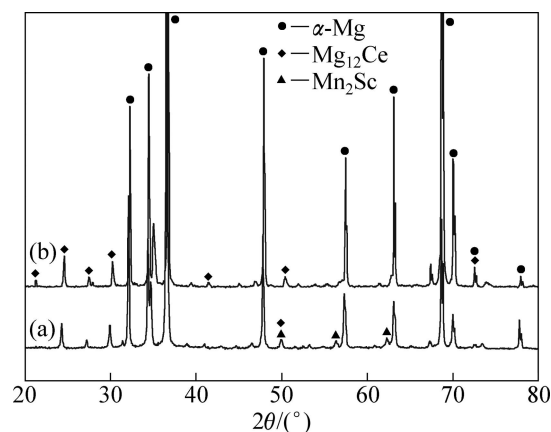
experimental alloys were measured from each elongation–time curve and averaged over three tests.

## 3 Results and discussion

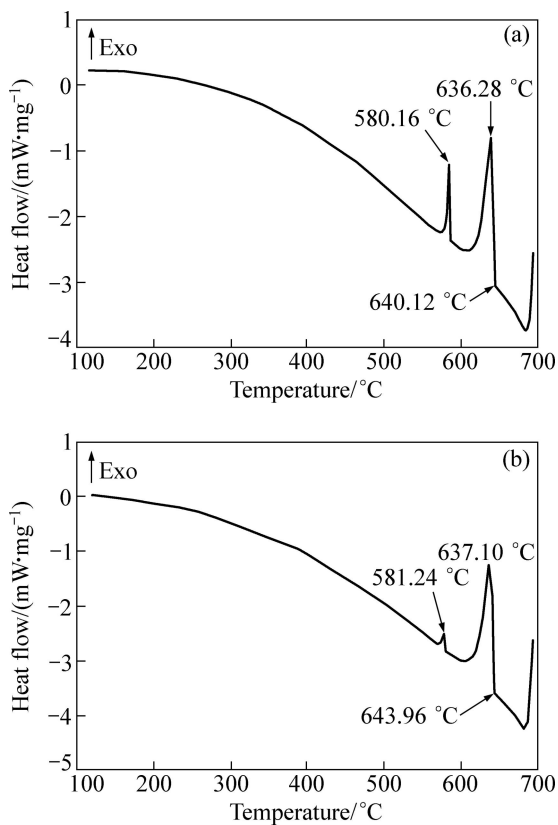
### 3.1 Comparison of microstructures

Figure 2 shows the XRD results of the as-cast alloys. In the Mg–3Ce–1.2Mn–0.9Sc alloy, two main phases have been reported in Ref. [9]. One is identified as Mn<sub>2</sub>Sc phase (hexagonal structure  $P6_3/mmc$ ,  $a=0.5033$  nm,  $c=0.8278$  nm), and the other one is Mg<sub>12</sub>Ce phase (tetragonal structure  $a=1.033$  nm,  $c=0.596$  nm). As shown in Fig. 2, the Sc-containing alloy is also mainly composed of  $\alpha$ -Mg, Mg<sub>12</sub>Ce and Mn<sub>2</sub>Sc phases. Furthermore, it is found from Fig. 2 that the Zn-containing alloy is mainly composed of  $\alpha$ -Mg and Mg<sub>12</sub>Ce phases, and the Mg–Zn phase which has been reported in the Mg–2.0Ce–0.7Zn–0.7Zr alloy by WU and XIA [10], is not identified in the alloy. The reason might be related to one of the following two aspects: 1) a small quantity of Mg–Zn phase formation is beyond detection limit for the spectrum of X-ray; 2) similar to the Mg–Zn–Y alloys [11], the Mg–Zn phase is not formed since the relatively low Zn/Ce ratio of the Zn-containing experimental alloy. Actually, the XRD results may be further confirmed by the DSC results of the as-cast alloys. Figure 3 shows the DSC cooling curves of the as-cast alloys. It is found from Fig. 3 that the DSC cooling curves of the two alloys are similar, with two main peaks in the cooling curves, corresponding to the  $\alpha$ -Mg matrix melting and the binary eutectic reaction ( $L_1 \rightarrow \alpha\text{-Mg} + \text{Mg}_{12}\text{Ce}$ ), respectively. Accordingly, the final microstructure of the two alloys mainly consists of  $\alpha$ -Mg and Mg<sub>12</sub>Ce phases. As for the Mn<sub>2</sub>Sc phase in the Sc-containing alloy, its formation has been described in detail in Refs. [2, 12].

Figures 4 and 5 show the optical images of the as-cast and solutionized alloys, respectively. It is observed from Fig. 4 that the primary  $\alpha$ -Mg phases in the



**Fig. 2** XRD results of as-cast alloys: (a) 1<sup>#</sup> alloy; (b) 2<sup>#</sup> alloy



**Fig. 3** DSC cooling curves of as-cast alloys: (a) 1<sup>#</sup> alloy; (b) 2<sup>#</sup> alloy

two alloys mainly display a dendrite configuration. Furthermore, it is found from Fig. 4 that the primary  $\alpha$ -Mg phases in the Sc-containing alloy are finer than those in the Zn-containing alloy, indicating that the Sc-containing alloy has finer grains than the Zn-containing alloy. This is further confirmed from Fig. 5 which shows the solutionized microstructures of the two alloys. The average grain sizes for the Sc- and Zn-containing alloys are 153  $\mu\text{m}$  and 196  $\mu\text{m}$ , respectively. Based on the Mg–Ce, Mg–Ce–Mn and Mg–Mn–Sc phase diagrams [3, 13, 14] and combined with the investigations of GROBNER and SCHMIOFETZER [12], during the solidification of the Mg–3Ce–1.2Mn–0.9Sc alloy, the primary  $\alpha$ -Mg phase and  $\text{Mn}_2\text{Sc}$  phase possibly first nucleate and grow until the temperature falls to about 585  $^{\circ}\text{C}$  where a binary eutectic reaction ( $L_1 \rightarrow \alpha\text{-Mg} + \text{Mg}_{12}\text{Ce}$ ) occurs. Obviously, the crystallizing temperature of the  $\text{Mn}_2\text{Sc}$  phase in the Mg–3Ce–1.2Mn–0.9Sc alloy is much higher than that of the eutectic phase ( $\alpha\text{-Mg} + \text{Mg}_{12}\text{Ce}$ ). Therefore, the formation of the  $\text{Mn}_2\text{Sc}$  will possibly induce the constitutional undercooling in a diffusion layer ahead of the advancing solid/liquid interface, which restricts the grain growth since the diffusion of the solute slowly occurs. In addition, further nucleation also possibly occurs in front of the interface because the nucleants in

the melt are more likely to survive and be activated in the constitutional undercooling zone, as reported by LEE et al [15] and FANG et al [16]. Based on the above analysis, it is preliminarily inferred that the reason why the Sc-containing alloy has finer grains than the Zn-containing alloy, is possibly related to the formation of the  $\text{Mn}_2\text{Sc}$  phase in the Sc-containing alloy.

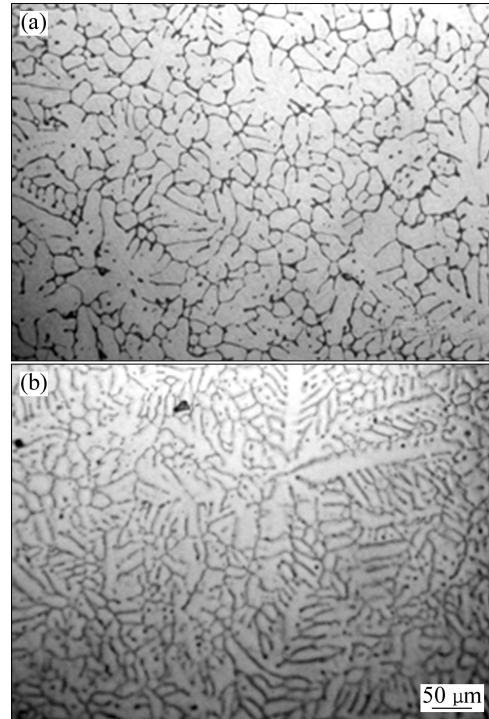


**Fig. 4** Optical images of as-cast alloys: (a) 1<sup>#</sup> alloy; (b) 2<sup>#</sup> alloy

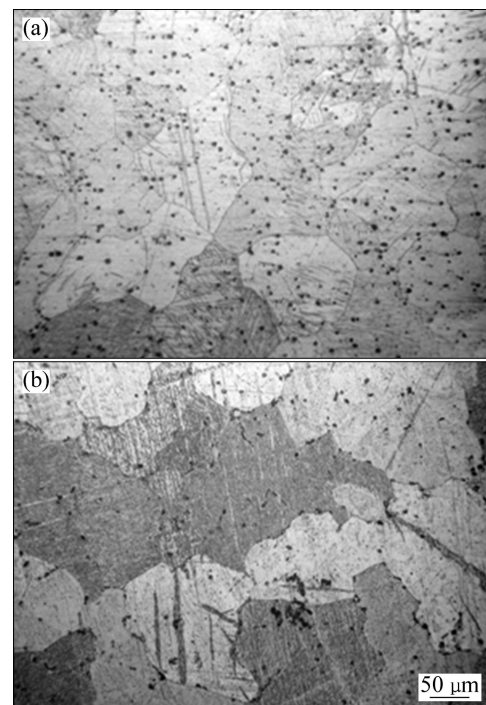


**Fig. 5** Optical images of solutionized alloys: (a) 1<sup>#</sup> alloy; (b) 2<sup>#</sup> alloy

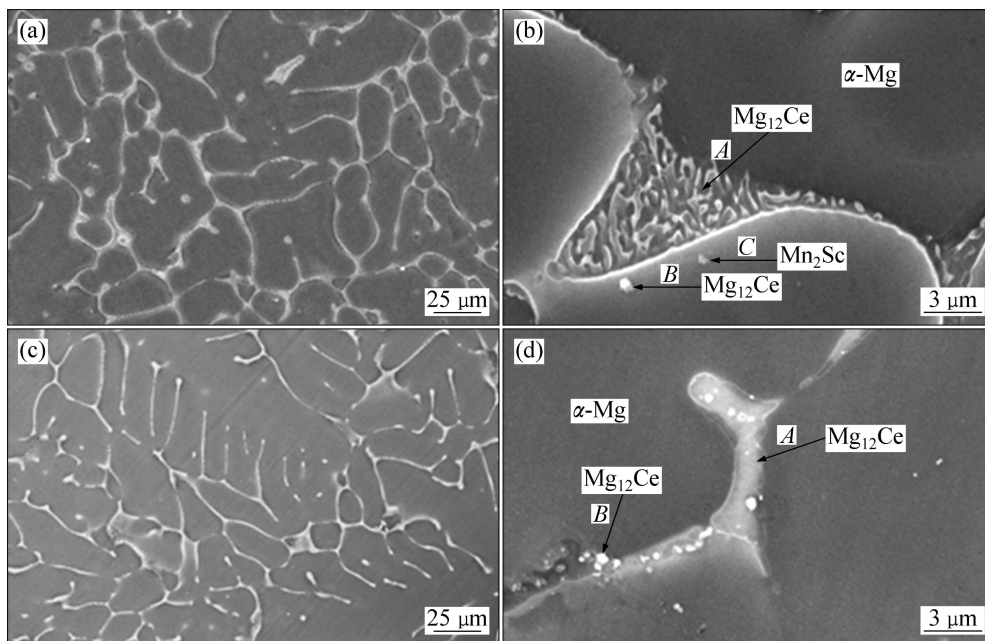
Figure 6 shows the SEM images of the as-cast alloys. In Fig. 6, the second phases in the as-cast alloys are identified according to the XRD and EDS results (Table 1). As shown in Figs. 6(a) and (b), it is found that the  $Mg_{12}Ce$  and  $Mn_2Sc$  phases in the Sc-containing alloy exhibit particle-like shapes, and the  $Mg_{12}Ce$  and  $Mn_2Sc$  phases mainly distribute at the grain boundary. In addition, it is further observed from Figs. 6(c) and (d) that the  $Mg_{12}Ce$  phases in the Zn-containing alloy mainly exhibit continuous and/or quasi-continuous nets. Of course, a small quantity of the  $Mg_{12}Ce$  phases with particle-like shapes are also observed (Fig. 6(d)). Similar to the distribution of the  $Mg_{12}Ce$  phases in the Sc-containing alloy, the  $Mg_{12}Ce$  phases in the Zn-containing alloy also distribute at the grain boundaries. Although the above results indicate that Zn in the Zn-containing alloy does not contribute to form any other phases. It is found from Table 1 that parts of Zn are located in the  $Mg_{12}Ce$  phase due to the strong attraction effects of Ce element [17]. Therefore, the  $Mg_{12}Ce$  phase in the Zn-containing alloy probably exists in the form of the  $(Mg,Zn)_{12}Ce$  intermetallic compound, as reported by KEVORKOV and PEKGULERYUZ [18]. However, this needs to be further confirmed.

**Table 1** EDS results of as-cast alloys

Position	w(Mg)/ %	w(Ce)/ %	w(Mn)/ %	w(Sc)/ %	w(Zn)/ %	Total/ %
A in Fig. 6(b)	77.67	22.33	–	–	–	100
B in Fig. 6(b)	83.77	16.23	–	–	–	100
C in Fig. 6(b)	70.95	–	18.36	10.69	–	100
A in Fig. 6(d)	78.91	17.31	–	–	3.78	100
B in Fig. 6(d)	80.89	19.11	–	–	–	100

### 3.2 Comparison of mechanical properties

The tensile properties including ultimate tensile strength (UTS), 0.2% yield strength (YS) and elongation (Elong.), and creep properties of the as-cast alloys are listed in Table 2. It is observed from Table 2 that, although the Sc- and Zn-containing alloys have similar as-cast tensile properties at room temperature and 300 °C, the Sc-containing alloy exhibits higher creep-resistant

**Fig. 6** SEM images of as-cast alloys: (a), (b) 1<sup>#</sup> alloy; (c), (d) 2<sup>#</sup> alloy**Table 2** Tensile and creep properties of as-cast alloys

Experimental alloy	Tensile property						Creep property at 300 °C and 30 MPa for 100 h	
	At room temperature			At 300 °C			Total creep strain/%	Minimum creep rate/ $10^{-8} s^{-1}$
	UTS/MPa	YS/MPa	Elong./%	UTS/MPa	YS/MPa	Elong./%		
1 <sup>#</sup> alloy	161 (3.1)	133 (1.9)	3.1 (0.25)	108 (2.1)	90 (1.8)	16.0 (0.89)	0.46 (0.10)	1.27 (0.39)
2 <sup>#</sup> alloy	152 (2.8)	130 (2.7)	3.0 (0.19)	101 (2.2)	87 (2.7)	15.6 (1.02)	1.85 (0.08)	5.14 (0.41)

Note: The data in the bracket are the standard error.

properties at 300 °C and 30 MPa for 100 h than the Zn-containing alloy. In general, it is accepted that the rate of dislocation creep tends to decrease with increasing grain size due to a lowered contribution of grain boundary sliding [19]. Since the grain size of the Sc-containing alloy is smaller than that of the Zn-containing alloy, the difference in the grain size can not explain the higher creep-resistant properties of the Sc-containing alloy than the Zn-containing alloy. The difference in the creep-resistant properties for the two alloys is possibly related to other reasons. Figure 7 shows the SEM images of the Sc- and Zn-containing solutionized alloys. It is observed from Fig. 7 that a majority of the  $Mg_{12}Ce$  phases in the two alloys have dissolved into the matrix after the solid solution heat treatment at 520 °C for 12 h. However, it is found that under the same solutionized conditions the amount of the remanent  $Mg_{12}Ce$  phases at the grain boundaries for the Sc-containing alloy seems to be relatively larger than that for the Zn-containing alloy. In addition, many fine and dispersed phases inside the grains of the Sc-containing solutionized alloy,  $Mg_{12}Ce$  and  $Mn_2Sc$ , are also observed. However, similar phenomenon is not

found inside the grains of the Zn-containing solutionized alloy. Obviously, the stability at high temperatures for the second phases in the Sc-containing alloy is possibly higher than the Zn-containing alloy. Since the creep-resistant properties of magnesium alloys are mainly related to the structure stability at high temperatures, it is preliminarily inferred that the higher creep-resistant properties of the Sc-containing alloy than the Zn-containing alloy are possibly related to the different initial as-cast microstructures of the two alloys. In spite of the above, the reason for the difference in the creep-resistant properties of the Sc- and Zn-containing alloys is not completely clear because some problems are still remained. For example, whether the  $Mg_{12}Ce$  phases in the Sc-containing alloy have really higher stability at high temperatures than those in the Zn-containing alloy? if yes, as shown in Fig. 6 and Table 1, whether the reason is related to the different morphologies and compositions of the  $Mg_{12}Ce$  phases in the two alloys? In addition, although the above results indicate that the as-cast creep-resistant properties of the Sc-containing alloy are higher than those of the Zn-containing alloy, one question whether the creep-resistant properties after an

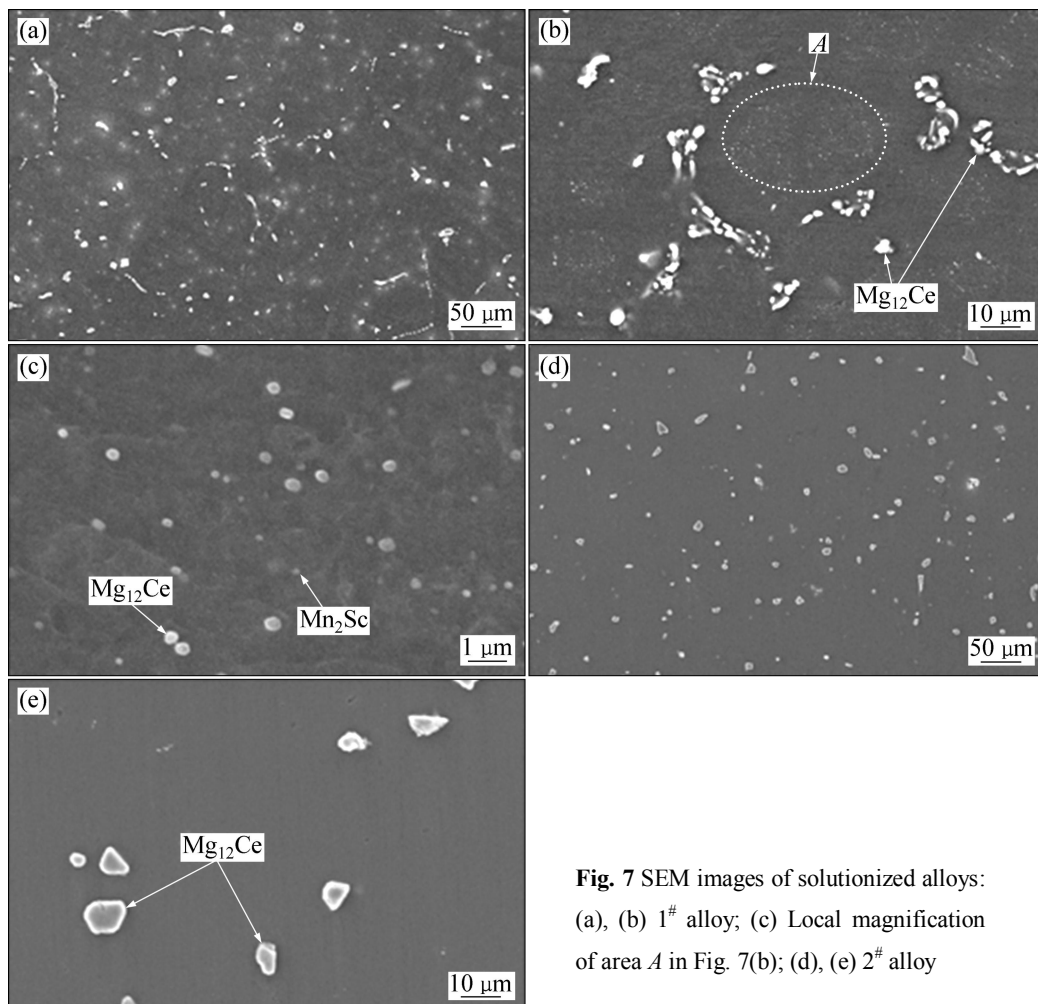


**Fig. 7** SEM images of solutionized alloys: (a), (b) 1<sup>#</sup> alloy; (c) Local magnification of area A in Fig. 7(b); (d), (e) 2<sup>#</sup> alloy

aging treatment for the Sc-containing alloy are higher than those for the Zn-containing alloy, still remains. These questions are a subject for further study in our group.

### 3.3 Comparison of fracture behaviour

Figure 8 shows the SEM images of tensile fractographs for the as-cast alloys failed in tensile test at room temperature. As shown in Fig. 8, a number of cleavage planes and steps are present, and some minute lacerated ridges can be observed in the localized areas of the tensile fracture surfaces for the two alloys, indicating that the tensile fracture surfaces of the Sc- and Zn-containing alloys have mixed characteristics of cleavage and quasi-cleavage fractures. Figure 9 shows the optical images of longitudinal sections for the as-cast alloys failed in tensile test at room temperature. It is observed from Fig. 9 that the tensile ruptures of the Sc- and Zn-containing alloys occur along inter-granular boundary. Therefore, it is preliminarily inferred that the Sc- and Zn-containing alloys have similar fracture mode. In spite of the above, a relatively obvious difference in the fracture surfaces of the Sc- and Zn-containing alloys is still observed from Fig. 8. As shown in Fig. 8, the directivity of the cleavage planes in the fracture surface of the Zn-containing alloy is more obvious than the Sc-containing alloy. The reason is possibly related to the different initial microstructures of the two as-cast alloys, especially the different morphologies of the  $Mg_{12}Ce$  phases in the two as-cast alloys.

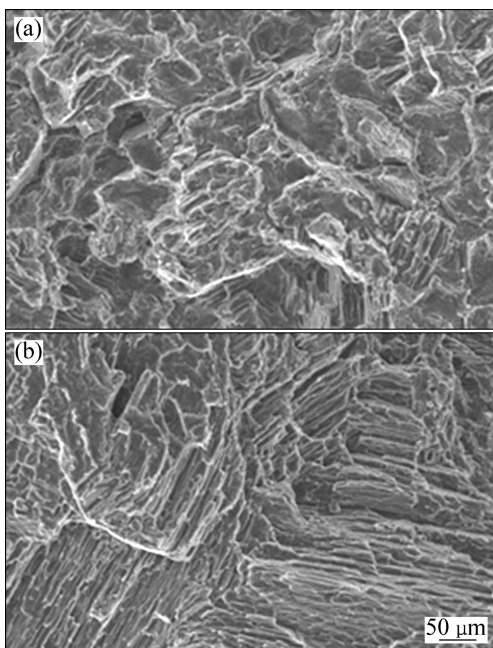


**Fig. 8** SEM images of tensile fractographs for as-cast alloys tested at room temperature: (a) 1<sup>#</sup> alloy; (b) 2<sup>#</sup> alloy

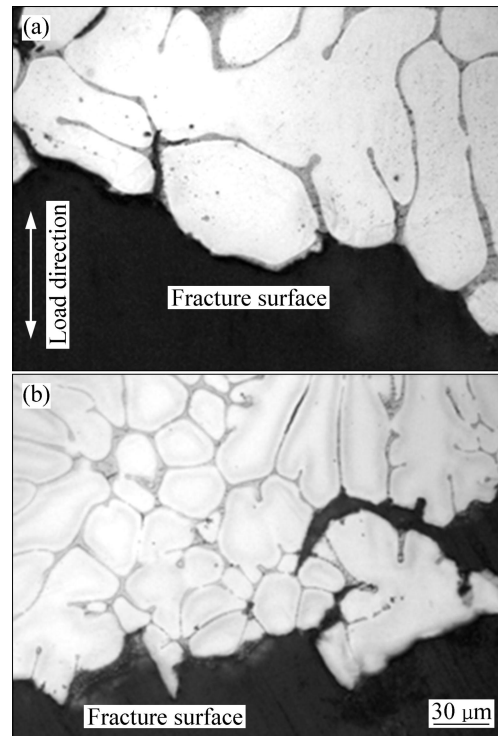


**Fig. 9** Optical images of longitudinal sections for as-cast alloys failed in tensile test at room temperature: (a) 1<sup>#</sup> alloy; (b) 2<sup>#</sup> alloy

## 4 Conclusions

1) The as-cast microstructure of the Mg–3Ce–1.2Mn–0.9Sc alloy mainly consists of  $\alpha$ -Mg,  $Mg_{12}Ce$  and  $Mn_2Sc$  phases, and the as-cast microstructure of the Mg–3Ce–1.2Mn–1Zn alloy is mainly composed of  $\alpha$ -Mg and  $Mg_{12}Ce$  phases.

2) The morphologies of the  $Mg_{12}Ce$  phases in the two as-cast alloys are different. The  $Mg_{12}Ce$  phase in the Sc-containing alloy mainly exhibits particle-like shapes. However, besides a small quantity of the particle-like  $Mg_{12}Ce$  phases, the  $Mg_{12}Ce$  phases in the Zn-containing alloy mainly exhibit continuous and/or quasi-continuous nets. Furthermore, the Sc-containing alloy has finer grains than the Zn-containing alloy.

3) In addition, although the Sc- and Zn-containing alloys have similar as-cast tensile properties at room temperature and 300 °C, the Sc-containing alloy exhibits higher creep-resistant properties at 300 °C and 30 MPa for 100 h than the Zn-containing alloy.

## References

- [1] PEKGULERYUZ M, CELIKIN M. Creep resistance in magnesium alloys [J]. *Inter Mater Reviews*, 2010, 55: 197–217.
- [2] MORDIKE B L, STULIKOVA I, SMOLA B. Mechanisms of creep deformation in Mg–Sc–based alloys [J]. *Metall Mater Trans A*, 2005, 36: 1729–1736.

- [3] BUCH F V, LIETZAU J, MORDIKE B L, PISCH A, SCHMID-FETZTER R. Development of Mg–Sc–Mn alloys [J]. Mater Sci Eng A, 1999, 263: 1–7.
- [4] ZHANG Xin-ming, PENG Zhuo-kai, CHEN Jian-mei, DENG Yun-lai. Heat-resistant magnesium alloys and their development [J]. The Chinese Journal of Nonferrous Metals, 2004, 14(9): 1443–1450. (in Chinese)
- [5] MORDIKE B L. Development of highly creep resistant magnesium alloys [J]. J Mater Proc Technol, 2001, 117: 391–394.
- [6] STULIKOVA I, SMOLA B, BUCH F V, MORDIKE B L. Mechanical properties and creep of Mg-rare earth-Sc-Mn squeeze cast alloys [J]. Materialwissenschaft und Werkstofftechnik, 2003, 34: 102–108.
- [7] SMOLA B, STULIKOVA I, PELCOVA J, MORDIKE B L. Significance of stable and metastable phases in high temperature creep resistant magnesium-rare earth base alloys [J]. J Alloys Compd, 2004, 378: 196–201.
- [8] SMOLA B, STULIKOVA I, PELCOVA J, ZALUDOVA N. Phase composition and creep behavior of Mg-RE-Mn alloys with Zn addition [C]//KAINER K U. Proceedings of 7th International Conference on Magnesium Alloys and Their Applications. Dresden: Wiley-VCH, 2007: 67–72.
- [9] SMOLA B, STULIKOVA I, PELCOVA J, BUCH F V, MORDIKE B L. Microstructure and phase changes due to heat treatment of squeeze cast Mg–Sc–(Ce)–Mn alloys [J]. Physica Status Solidi (a), 2002, 191: 305–316.
- [10] WU Wen-hua, XIA Chang-qing. Microstructures and mechanical properties of Mg–Ce–Zn–Zr wrought alloy [J]. Journal of Central South University of Technology, 2004, 11(4): 367–370.
- [11] LEE J Y, KIM D H, LIM H K, KIM D H. Effects of Zn/Y ratio on microstructure and mechanical properties of Mg–Zn–Y alloys [J]. Mater Letters, 2005, 59: 3801–3805.
- [12] GROBNER J, SCHMID-FETZTER R. Selection of promising quaternary candidates from Mg–Mn–(Sc, Gd, Y, Zr) for development of creep-resistant magnesium alloys [J]. J Alloys Compd, 2001, 320: 296–301.
- [13] KANG Y B, PELTON A D, CHARTRAND P, SPENCER P, FUERST C D. Thermodynamic database development of the Mg–Ce–Mn–Y system for Mg alloy design [J]. Metall Mater Trans A, 2007, 38: 1231–1243.
- [14] ZHANG H X, KEVORKOV D, JUNG I H, PEKGULERYUZ M. Phase equilibria on the ternary Mg–Mn–Ce system at the Mg-rich corner [J]. J Alloys Compd, 2009, 482: 420–428.
- [15] LEE Y C, DAHLE A K, STJOHN D H. The role of solute in grain refinement of magnesium [J]. Metall Mater Trans A, 2000, 31: 2895–2906.
- [16] FANG X Y, YI D Q, NIE J F, ZHANG X J, WANG B, XIAO L R. Effect of Zr, Mn and Sc additions on the grain size of Mg–Gd alloy [J]. J Alloys Compd, 2009, 470: 311–316.
- [17] SHIN B S, KOOK J W, BAE D H. Microstructure and deformation behavior of a Mg–RE–Zn–Al alloy reinforced with the network of a Mg–RE phase [J]. Met Mater Int, 2009, 15: 203–207.
- [18] KEVORKOV D, PEKGULERYUZ M. Experimental study of the Ce–Mg–Zn phase diagram at 350 °C via diffusion couple techniques [J]. J Alloys Compd, 2009, 478: 427–436.
- [19] ZHU S M, MORDIKE B L, NIE J F. Creep properties of a Mg–Al–Ca alloy produced by different casting technologies [J]. Mater Sci Eng A, 2008, 483–484: 583–586.

## Mg–3Ce–1.2Mn–0.9Sc 和 Mg–3Ce–1.2Mn–1Zn 镁合金 铸态组织和力学性能的比较

杨明波<sup>1,2,3</sup>, 潘复生<sup>3</sup>

1. 重庆理工大学 材料科学与工程学院, 重庆 400054;
2. 重庆理工大学 汽车零部件制造及检测教育部重点实验室, 重庆 400054
3. 重庆大学 国家镁合金材料工程研究中心, 重庆 400030

**摘要:** 比较研究了 Mg–3Ce–1.2Mn–0.9Sc 和 Mg–3Ce–1.2Mn–1Zn 镁合金的铸态组织和力学性能。结果表明: 含 Sc 合金主要由  $\alpha$ -Mg、Mg<sub>12</sub>Ce 和 Mn<sub>2</sub>Sc 相组成, 而含 Zn 合金则主要由  $\alpha$ -Mg 和 Mg<sub>12</sub>Ce 相组成。然而, 含 Sc 和含 Zn 铸态合金中 Mg<sub>12</sub>Ce 相的形貌是不同的。含 Sc 合金中的 Mg<sub>12</sub>Ce 相主要呈颗粒状, 而含 Zn 合金中的 Mg<sub>12</sub>Ce 相则主要呈连续和/或准连续的网状。同时, 含 Sc 合金的晶粒较含 Zn 合金的相对较为细小。此外, 虽然含 Sc 合金和 Zn 合金在室温和 300 °C 下具有相似的抗拉性能, 但含 Sc 合金在 300 °C 和 30 MPa 下持续 100 h 后的抗蠕变性能较 Zn 合金的好。

**关键词:** 镁合金; Mg–Ce–Mn 基合金; Sc; Zn; Mg<sub>12</sub>Ce 相

(Edited by YANG Hua)